Exploring linker's sequence diversity to fuse carotene cyclase and hydroxylase for zeaxanthin biosynthesis

Aurélie Bouin, Congqiang Zhang, Nic Lindley, Gilles Truan, Thomas Lautier

Metabolic Engineering Communications 16 (2023) e00222

Contents lists available at ScienceDirect

Metabolic Engineering Communications

journal homepage: www.elsevier.com/locate/mec

Exploring linker's sequence diversity to fuse carotene cyclase and hydroxylase for zeaxanthin biosynthesis

Aurélie Bouin [a,b], Congqiang Zhang [a,**], Nic D. Lindley [a,b], Gilles Truan [b,***], Thomas Lautier [a,b,c,*]

[a] Singapore Institute of Food and Biotechnology Innovation (SIFBI), Agency for Science, Technology and Research (A*STAR), Singapore
[b] TBI, Université de Toulouse, CNRS, INRAE, INSA, Toulouse, France
[c] CNRS@CREATE, 1 Create Way, #08-01 Create Tower, 138602, Singapore

ARTICLE INFO

Handling Editor: Mattheos Koffas

Keywords:
Zeaxanthin
Linker
Artificial protein fusion
Protein engineering

ABSTRACT

Fusion of catalytic domains can accelerate cascade reactions by bringing enzymes in close proximity. However, the design of a protein fusion and the choice of a linker are often challenging and lack of guidance. To determine the impact of linker parameters on fusion proteins, a library of linkers featuring various lengths, secondary structures, extensions and hydrophobicities was designed. Linkers were used to fuse the lycopene cyclase (crtY) and β-carotene hydroxylase (crtZ) from *Pantoea ananatis* to create fusion proteins to produce zeaxanthin. The fusion efficiency was assessed by comparing the carotenoids content in a carotenoid-producer *Escherichia coli* strain. It was shown that in addition to the orientation of the enzymes and the size of the linker, the first amino acid of the linker is also a key factor in determining the efficiency of a protein fusion. The wide range of sequence diversity in our linker library enables the fine tuning of protein fusion and this approach can be easily transferred to other enzyme couples.

1. Introduction

Carotenoids are tetraterpenoid pigments commonly found in bacteria, fungi, algae and plants. Carotenoids act as antioxidants and are responsible for light absorption in photosynthetic organisms (Zakynthinos and Varzakas, 2016). Among carotenoids, zeaxanthin is a xanthophyll giving to corn or egg yolk their characteristic yellow colour (Sajilata et al., 2008). It is also known as colourant E161h in the food industry and used as a feed additive for fish and poultry (Sajilata et al., 2008). Moreover, zeaxanthin is also used as a dietary supplement for human eye health. Indeed, zeaxanthin and lutein are the only two carotenoids found in the vicinity of the human retina where they have a putative preventive effect against macular degeneration (Arunkumar et al., 2020). By 2030, the market demand for zeaxanthin is expected to reach US$ 210 Million (Zafar et al., 2021).

Zeaxanthin can be produced by chemical synthesis. However, organic synthesis typically produces racemic mixtures, and only specific isomers present a biological activity, such as the 3R,3′R-zeaxanthin and 3R,3′S-RS- zeaxanthin in the retina (Mares, 2016). The environmental impact of the chemical synthesis is also incompatible with the required sustainable production, which needs to adopt an ecological integrative workflow as described in the One Health paradigm from the World Health Organisation (Mackenzie and Jeggo, 2019). Zeaxanthin can also be extracted from natural producers such as the marigold flowers (Barreiro and Barredo, 2018) or maize (OLIVEIRA et al., 2013) but this method is limited by its low yield. An alternative way to produce biomolecules is by microbial fermentation. Zeaxanthin can be produced in both natural and genetically engineered microorganisms (Y. Zhang et al., 2018). Production of high-value compounds such as zeaxanthin via metabolic engineering is a serious alternative to the other two methods (extraction from natural producers and chemical synthesis) because microbial fermentation processes use renewable feedstocks, is safer and environment-friendly (Rinaldi et al., 2022). Engineered microbial approach offers tools to optimize the production and to diversify the type of products. However, challenges remain to design robust microbial strains, involving protein and metabolic engineering, and to

* Corresponding author. Singapore Institute of Food and Biotechnology Innovation (SIFBI), Agency for Science, Technology and Research (A*STAR), Singapore.
** Corresponding author.
*** Corresponding author.
E-mail addresses: zcqsimon@outlook.com (C. Zhang), gilles.truan@insa-toulouse.fr (G. Truan), thomas.lautier@cnrs.fr (T. Lautier).

https://doi.org/10.1016/j.mec.2023.e00222
Received 14 March 2023; Received in revised form 12 April 2023; Accepted 16 April 2023
Available online 24 April 2023

establish an efficient bioprocess including fermentation and downstream product purification.

In the engineered *Escherichia coli* strain producing zeaxanthin, the two terpenoid precursors, isopentenyl diphosphate (IPP) and dimethylallyl diphosphate (DMAPP) are produced by implementing the heterologous mevalonate pathway to supplement the prokaryotic endogenous non-mevalonate pathway. The terpenoid building blocks are then successively assembled into lycopene and both extremities of lycopene are cyclised by the β-carotene cyclase (crtY) to form β-carotene. Zeaxanthin is produced from β-carotene by a hydroxylation step on each of the β-carotene rings, on position 3 and 3'. The enzyme responsible for the reaction is the β-carotene hydroxylase, crtZ.

Previous efforts for the production of zeaxanthin in *E. coli* include a study on the most efficient gene arrangement of zeaxanthin gene pathway on an operon (Nishizaki et al., 2007), the use of tunable intergenic region (TIGR) to adjust individually the expression of crtY and crtZ genes (Li et al., 2015), the regulation of the mevalonate pathway using dynamically control TIGR approach (Shen et al., 2016), the optimization of the initial codon in zeaxanthin pathway genes (Wu et al., 2019) and the multidimensional regulation of genes grouped into modules (Chen et al., 2021). *Saccharomyces cerevisiae* (Carquet et al., 2015), the red yeast *Xanthophyllomyces dendrorrhous* (Breitenbach et al., 2019; Pollmann et al., 2017) and *Yarrowia lypolitica* (Xie et al., 2021) have also been engineered for the production of zeaxanthin. These studies focus on the modulation of gene expression level to achieve pathway efficiency. However, β-carotene is never fully converted into zeaxanthin and the concentrations of zeaxanthin obtained are not economically viable yet.

A complementary approach to the transcriptional regulation is to improve the pathway efficiency through enzymatic spatial organisation, by bringing enzymes of the same metabolic pathway in close proximity. Indeed, spatial proximity of enzymes is thought to improve reaction velocity by reducing diffusion of intermediates and increasing local concentration of enzymes and substrates (Qiu et al., 2018). Spatial optimization can be achieved at different scales. Microcompartments allow for the sequestration of enzymes and hydrogenases have previously been targeted in a repurposed carboxysome (Li et al., 2020). Synthetic scaffolds made of proteins or nucleic acids are widely used to anchor enzymes (Geraldi et al., 2021; Park et al., 2022). Finally, at a scale limited to two or three enzymes, protein fusions allow to bring enzymes together in a one-to-one ratio (Elleuche, 2015).

Protein fusions are made of at least two protein domains. A linker joining both domains is often required to maintain a proper protein folding while allowing domain interactions (Wriggers et al., 2005). Linker characteristics were studied in natural multidomain proteins in terms of length, conformation and amino acid composition (Argos, 1990; George and Heringa, 2002). More recently, the role of the linker flexibility (Li et al., 2016; Van Rosmalen et al., 2017), cloning strategies for a wide selection of linkers between proteins (Gräwe et al., 2020; Norris and Hughes, 2018) and linkers for membrane proteins (Sadaf et al., 2016) were studied on artificial protein fusions, however, the impact of the linker's sequence on the fusion efficiency was not analysed and there is a lack of knowledge to predict which linker sequence will lead to a functional enzymatic fusion.

In this study, a protein-fusion approach was conducted to increase the production of zeaxanthin in an engineered *Escherichia coli* strain. To reduce the accumulation of the intermediate, β-carotene, the last two enzymes of the zeaxanthin pathway, crtY and crtZ were fused. The enzyme fusion was optimised by testing a collection of linkers, shortlisted according to idiosyncratic properties. In the end, we provided insight regarding the design of protein fusion and discussed the limitations of the approach.

2. Materials and methods

2.1. Strain and plasmid

E. coli Bl21-Gold DE3 strain (Stratagene) was used in this study. The plasmids p15A-spec-hmgS-atoB-hmgR, p15A-cam-mevK-pmk-pmd-idi, p15A-kan-crtEBI-ispA, p15A-crtYZ and p15a-crtY were obtained from a previous study (Zhang et al., 2018b) and the resulting lycopene producing strain was used as a platform to produce zeaxanthin (Fig. 1). p15Aamp-crtZY plasmid was obtained by insertion of CrtZ gene in p15A-crtY plasmid.

2.2. Construction of the linker library

The linkers were cloned based on a generic plasmid using a method inspired from golden gate cloning. To insert the linkers sequences, a SapI restriction site was inserted between the sequences of crtY and crtZ in p15Aamp-crtYZ and p15Aamp-crtZY plasmids. The digestion of the vectors by SapI enzyme from New England Biolabs (NEB) resulted in opened plasmids with 3 bases overhang on each side.

The creation of the linker library was achieved by designing primers combining the sequence of the linker plus three nucleic acids complementary to the one of the SapI overhang sequences. Primer couples were mixed into water, heated at 70 °C for 5 min and slowly cooled down at room temperature to allow annealing of matching sequences and obtain

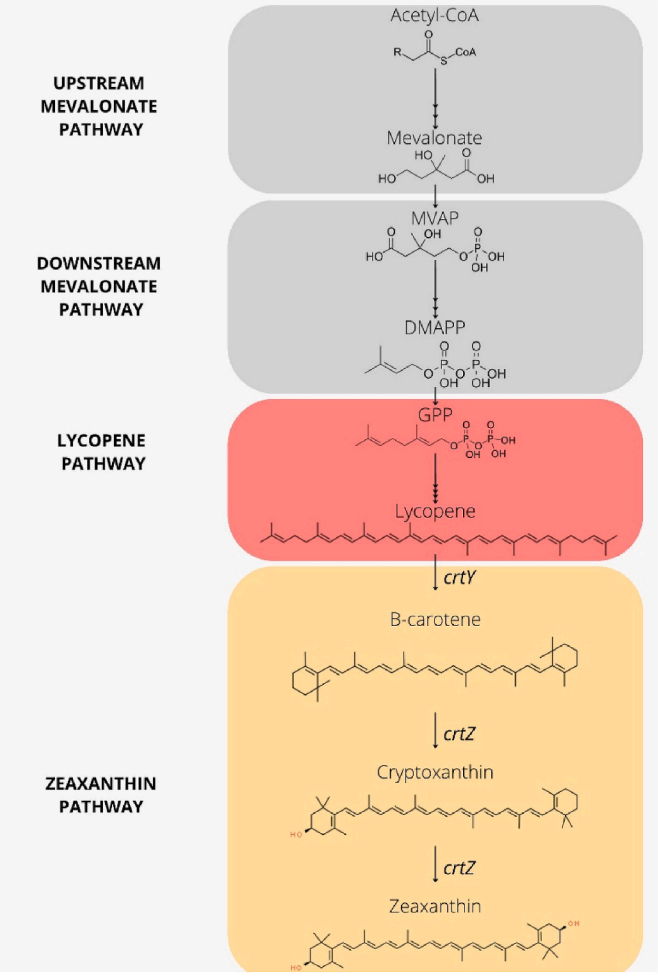

Fig. 1. Metabolic pathway of zeaxanthin. Each block represents a module of a set of genes clustered on one plasmid (Zhang et al., 2018b). MVAP: phosphomevalonate; DMAPP: dimethylallyl pyrophosphate; GPP: geranyl pyrophosphate.

double stranded DNA. The double stranded DNA of the linker, with 3 bp overhang, was then ligated with T4 DNA ligase in the SapI digested plasmids to obtain p15A-amp-crtY-linker-crtZ and p15Aamp-crtZ-linker-Y plasmids. Correct plasmids identified by sequencing were transformed in the *E. coli* K12 MG1655 producing strain with the three plasmids harbouring the mevalonate and lycopene pathway genes.

2.3. Culture conditions

After an overnight preculture in 2XPY medium (20 g/L peptone, 10 g/L yeast extract and 10 g/L NaCl), cells were inoculated at OD600nm = 0.1 in 2XPY medium supplemented with 20 g/L glycerol, 50 mM 4-(2-hydroxyethyl)- 1-piperazineethanesulfonic acid (HEPES) and Tween 80 0.5%, as previously described (Zhang et al., 2018a). The cells were grown at 37 °C and 250 rpm until OD600nm reached ~0.8, they were then induced by addition of 0.05 mM IPTG and were grown at 30 °C for 24 h. Antibiotics (34 μg/ml chloramphenicol, 50 μg/ml kanamycin, 50 μg/ml spectinomycin and 100 μg/ml ampicillin) were added to the culture to maintain the four plasmids.

2.4. Extraction and quantification of carotenoids

Total intracellular carotenoids were extracted from cellular pellets according to the acetone extraction method (Zhang et al., 2018a). Briefly, 20 μL of bacterial culture were centrifuged for 10 min at 14000 g. The cell pellets were resuspended in 200 μL of acetone. After a 20 min incubation at 50 °C and 1500 rpm, the mixture was centrifuged for 10 min at 14000 g. The supernatant was filtered using a PTFE, 0.45 μm filter and subjected to HPLC analysis carried out by an Agilent 1260 Infinity LC system equipped with a ZORBAX, Eclipse Plus C18, 4.6 × 250 mm, 5 μm column and diode array detector (DAD). Isocratic conditions (80% acetonitrile, 18% methanol, and 2% water) were maintained at 1 mL/min for 10 min for all experiments except for linker mutation analysis. The run concerning the linker mutation analysis was performed using a more separative gradient starting at 48% methanol, 12% water and 40% acetonitrile and lasting 1 min. For the next 3 min, a gradient was applied to reach 16% methanol, 4% water and 80% acetonitrile, until the end of the run. The entire run lasted 10 min. The carotenoids were detected and quantified through absorbance at 450 nm. Standard curves were generated using chemically synthesised lycopene, β-carotene, β-cryptoxanthin and zeaxanthin (CaroteNature, Switzerland).

For the time-course profile experiment, the usual ratio 1:10 of cell to solvent was adjusted between 2:1 to 1:10 along the experiment to allow the extraction and detection of smaller amounts of carotenoids.

2.5. SDS-PAGE

SDS-PAGE analysis was carried out on BL21 strain only carrying the last module plasmid (p15a-Amp either empty, or with crtY gene or crtZ-crtY gene fusion). 10 mL of culture were centrifuged at 4000g for 10 min at 4 °C. Cell pellets were concentrated 10 times in 1 mL of buffer I (200 mM Tris Hcl, 50 mM NaCl, 1 mg/ml lysozyme and 1x protease inhibitor) and incubated for 30 min at 4 °C. Cells were then lysed by 3 cycles of freeze-thawing. DNAse at 1.5 μl/ml and 2 mM $MgCl_2$ were then added to the lysate mixture. Protein concentration was determined by BCA assay. 6 μL of sample containing 10 μg of protein were mixed with 1 μl of 10X reducing agent (Invitrogen™ NuPAGE™) and 2.5 μl of 4x loading buffer (Invitrogen™ NuPAGE™). Samples were loaded on SDS-PAGE gel with 4–12% polyacrylamide gradient and run at 180V until the migration front reached the end on the gel. Proteins were detected by Coomassie blue staining.

2.6. Statistics

Rstudio software (version Rstudio/2022.12.0 + 353) was used for statistical analysis. One-way ANOVA was used to compare one independent factor in three independent groups. Two-way ANOVA was used to compare two independent factors in four independent groups. When the ANOVA was significant, the Tukey post Hoc test or *t*-test were used to make pairwise comparisons between groups. The normality of variance (shapiro test) and homogeneity of variance (Levene's test) were verified for all ANOVA analysis. When the aforementioned hypotheses were not verified, a logarithmic transformation was applied to the variable. P-values were calculated and represented as follow: $P < 0.05$, $P < 0.01$, $P < 0.001$ and $P < 0.0001$ were indicated by *, **, *** and **** respectively. Only significant differences were indicated.

3. Results

3.1. The orientation of the fused enzymes crtY and crtZ is crucial for their activities

To establish the importance of the enzyme order in the fused assembly crtY/crtZ, the enzymes were fused in both orientations with synthetic linkers typically used in literature (Li et al., 2016). The linkers were constituted of one to four repeats of either the flexible motif (GGGGS) or the rigid spacer (EAAAK). The fifteen resulting plasmids expressing the independent or fused crtY/crtZ couples were transformed in the lycopene producing strain to reconstitute a full zeaxanthin pathway. The control strain with independent enzymes (EAB09) accumulated around forty percent of the β-carotene precursor while the final product zeaxanthin represented fifty percent of the total carotenoids.

The first orientation consisted of fusing the C-terminal of crtY to the linker, leading to a set of crtY-linker-crtZ fusions. In the case of the crtY-$(EAAAK)_x$-crtZ fusions, lycopene is accumulated and a small amount of β-carotene is detected (Fig. 2A). Fusing the C-terminal of crtY with GGGGS linkers restore the β-carotene production to a level comparable to the control strain EAB09. The amount of β-carotene accumulated gradually increased with the size of the linker. Independently of the linker type, these results indicated that crtY activity is affected by its order in the fusion. The amino acid sequences of crtY and crtZ were analysed to identify the presence of a transmembrane domain using the web-server Phobius (Madeira et al., 2019). AlphaFold predicted structures of both crtY and crtZ were retrieved from AlphaFoldDB (Fig. S1).

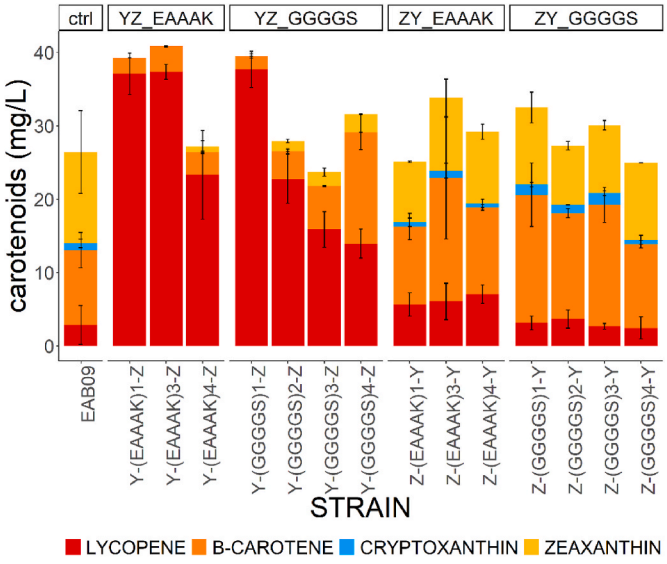

Fig. 2. A: Carotenoids content in mg/L of the strains harbouring the fusion constructs Y-linker-Z and Z-linker-Y. EAB09 is the control (ctrl) strain expressing independent enzymes. Errors bars represent the standard deviation of two independent experiments. The control strain experiment was repeated four times.

Phobius web-server did not predict any transmembrane domain for crtY, and the predicted Alphafold structure is rather globular. We thus hypothesize that prokaryotic crtY from *Pantoea ananatis* is more likely a membrane-associated protein rather than anchored to the membrane unlike eukaryotic isoforms of crtY (Krubasik and Sandmann, 2000; Rabeharindranto et al., 2019). Indeed, the expression of crtY from *P. ananatis* was previously optimised by fusion to a N-terminal Maltose Binding Protein (MBP) tag suggesting that membrane location for crtY in *E. coli* is favourable (Yu et al., 2010). Regarding the zeaxanthin production, even if more β-carotene is accumulated, very little zeaxanthin is produced, giving the impression that crtZ activity is also impeded in this orientation. This would be consistent with previous studies (Ding et al., 2022; Henke and Wendisch, 2019; Nogueira et al., 2019; Wu et al., 2019) where fusion proteins with crtZ placed at the C-terminal of the construct were not producing zeaxanthin. The Phobius prediction shows three transmembrane helices at the N-terminal of crtZ, with the N-terminal orientated toward the extracellular space. The fusion of crtY enzyme at the N-terminal of crtZ could thus impede the correct orientation of crtY towards the membrane and its access to the substrate, leading to the accumulation of the substrate of crtY, lycopene in the crtY-crtZ fusions. We hypothesized that crtY require a long and flexible linker (crtY-$(GGGGS)_4$-crtZ) to compensate an unfavourable first location in the crtY-crtZ fusion. Surprisingly, strains with unfunctional crtY protein (crtY-$(EAAAK)_x$-crtZ), had a significantly higher production of lycopene (or total carotenoids) than the strains producing the downstream products β-carotene and zeaxanthin. The decrease in total carotenoid production in presence of functional crtY and crtZ enzymes might be due to the consumption of cofactor in the cell. Indeed, crtY has been shown to consume NADH and NADPH (Yu et al., 2010) and crtZ, NADPH (Bouvier and Keller, 1998).

The second orientation consisted of the C-terminal of crtZ fused to the linker, leading to a set of crtZ-linker-crtY fusions. Independently of the linker motif, all crtZ-crtY fusions were able to produce β-carotene and zeaxanthin to a level similar to the one of the non-fused enzymes (Fig. 2A). According to these first results, the crtZ-crtY orientation was chosen to further characterise and improve the crtZ-crtY protein fusion. As differences were observed based on the size and motifs of the linkers, exploring the sequences of the linkers could lead to optimize the fusion efficiency and was assay by building a linker library.

3.2. Conception of a linker library

To optimize the crtZ-crtY protein fusion, a library of 91 linkers was designed out of the 1280 present in the online linker database IBIVU, based on natural linkers from natural multidomain proteins (George and Heringa, 2002). The 91 linkers were selected to conserve a proportion of linkers by category similar to the one in the online database. Each linker of the pool was annotated using four criteria: size, structure, C-alpha extent and hydrophobicity (Fig. 3). For the size, 3 classes were designed. Small linkers contain from two to five amino acids (notated S), medium linkers are between six and thirteen amino acids (notated M) and large linkers between fourteen to fifty-eight amino acids (notated L). The linker structure can either be helical (notated H) or non-helical (notated N). The extension of the linker, C-alpha extent, is defined by the average distance between its amino acids divided by the number of amino acids minus one. Two classes of C-alpha extent were designed: those with an average inferior to 2 Å (notated I) and those with an average superior to 2 Å (notated S). Lastly, linkers are ranged by their average hydrophobicity according to the Eisenhower scale. For example, the MHI05 linker is a Medium size linker, Helical, with a C-alpha extent Inferior to 2 Å. It is more hydrophobic than MHI04 but less hydrophobic than MHI06.

3.3. Small linkers improve pathway efficiency

To optimize the size of the linker in the crtZ-crtY fusion protein, four linkers of each size's class (small, medium and large) were cloned between crtZ and crtY and the carotenes content was quantified in the 12 strains. All strains displaying a crtZ-crtY fusion construct with a linker produced a similar amount of carotenoid to the strain EAB09 expressing the non-fused enzymes. This indicates that all linkers lead to a functional fusion, although the overall carotenoid production was not improved (Fig. 4A). To refine the impact of the linkers, the ratio of xanthophylls and carotenes, reflecting the efficiency of the pathway to produce final metabolites, was compared between strains expressing different sizes of linker in the fusion protein (Fig. 4B). Strains expressing a small or medium linker between crtZ and crtY had a 1.8-fold increase of their ratio of xanthophylls compared to the control strain and the strain with large linkers. Strains harbouring large linkers accumulate more precursors (lycopene or β-carotene) than the non-fused construct. The balance of pathway intermediates is then modified based on the linker size, with the more favourable ratio involving the small linkers. The size effect between crtY and crtZ could be due to folding issues or linker proteolysis effects, favoured in the longer class. Another hypothesis could be that a small linker will create a compact and more stable enzymatic complex, closer to the membrane, where lycopene, the hydrophobic substrate, could be more accessible for crtY. Thus, small linkers were chosen to further optimize the crtZ-crtY fusion.

SIZE	Helical	C-alpha extent category	Number of linker	Proportion
LARGE			19	21%
	Helical		8	9%
		<2 Å	7	8%
		>2 Å	1	1%
	non helical		11	12%
		<2 Å	9	10%
		>2 Å	2	2%
MEDIUM			52	57%
	Helical		28	31%
		<2 Å	17	19%
		>2 Å	11	12%
	non helical		24	26%
		<2 Å	13	14%
		>2 Å	11	12%
SMALL			20	22%
	Helical		7	8%
		<2 Å	2	2%
		>2 Å	5	5%
	non helical		13	14%
		<2 Å	2	2%
		>2 Å	11	12%
TOTAL			**91**	**100%**

Fig. 3. Classification of the linker properties and their repartition in the library. Heading in dark grey give the category of the linker. Sub-headings in light grey represents a class within the category and numbers in these lines represent the sub total of linkers in each class.

3.4. crtZ-crtY fusions with small linkers show diverse carotenoids profiles

To assess the role of linkers physical parameters in crtZ-linker-crtY fusions, nineteen small linkers from the linker library were selected and cloned between both enzymes. Although composed of only three to five amino acids, linkers were described in the database presenting a range of flexibility, extension or hydrophobicity different from one another. The carotenes content was quantified in the nineteen resulting strains as well as in the strain with the non-fused enzyme, EAB09. The amounts of carotenoids produced in each strain is shown in Fig. 5A, strains are grouped by the category of the linkers in the enzyme fusion, and strains are ranged by ascending order of total carotenoids amounts

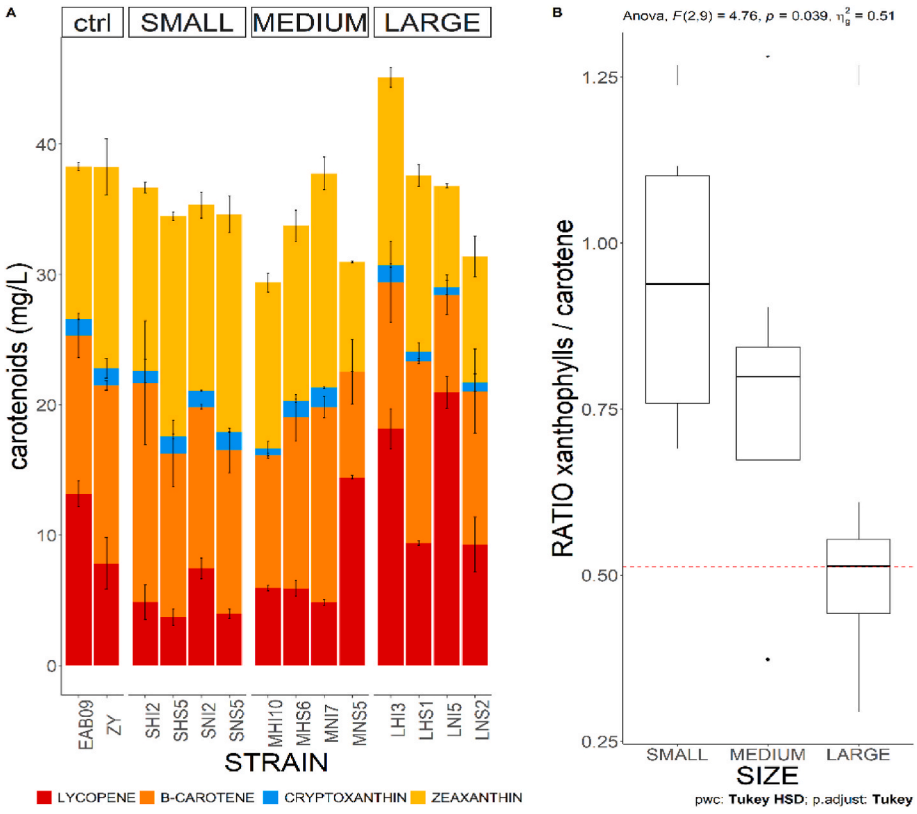

Fig. 4. A: Carotenoid content in mg/L of the strains harbouring the fusion constructs Z-linker-Y with small, medium or large linkers. EAB09 is the control strain with non-fused enzymes. ZY is the strain with enzymes fused directly, without linker. Errors bars represent the standard deviation of two independent experiments. **B:** Ratio of xanthophylls to carotenes with the strains clustered according to the size of the linker. Data is presented as standard boxplots. Dark bars represent median values, boxes are the range from first to third quartile, whiskers represent minima and maxima. The dashed red line represents the ratio of xanthophylls to carotenes in the strain with independent enzymes (strain EAB09). (For interpretation of the references to colour in this figure legend, the reader is referred to the Web version of this article.)

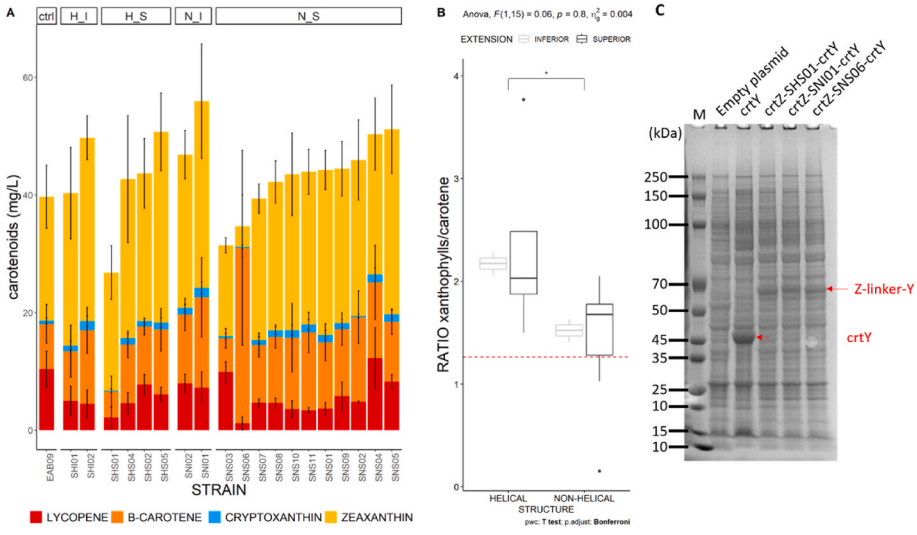

Fig. 5. A: Carotenoid content in mg/L of the strains harbouring the fusion constructs crtZ-linker-crtY with small linkers. EAB09 is the control strain with non-fused enzymes. Errors bars represent the standard deviation of two independent experiments. N_I: NON-HELICAL_INFERIOR; H_I: HELICAL_INFERIOR; H_S: HELICAL_SUPERIOR; N_S: NON-HELICAL_SUPERIOR. Non-helical and helical refers to the presumed secondary structure of the linker while inferior and superior refers to the extension of the linker. Among each category, strains are ranged by ascending order of total amount carotenoids. **B:** Ratio of xanthophylls to carotenes with the strains clustered according to the structure and extension of the linker. Data are presented as standard boxplots. Dark bars represent median values, boxes are the range from first to third quartile, whiskers represent minima and maxima. The dashed red line represents the ratio of xanthophylls to carotenes in the strain with independent enzymes (strain EAB09). **C:** SDS-PAGE of BL21 strain containing the final plasmid of the pathway with an empty vector, crtY enzyme, fusion enzymes crtZ-SHS01-crtY, crtZ-SNI01-crtY, crtZ-SNS06-crtY. M indicates the line with protein molecular weight marker. Red arrow indicates the proteins of interest. (For interpretation of the references to colour in this figure legend, the reader is referred to the Web version of this article.)

(Fig. 5A). Among the nineteen protein fusions with small linkers, eighteen were functional, as zeaxanthin is produced in the correlated strain. Although most strains displayed a similar profile of carotenoid accumulated, a few stood out from the others. First, the strain having the crZ and crtY enzyme fused together with the SNS06 linker accumulated only β-carotene, with lycopene precursor being almost fully converted to β-carotene and little to no zeaxanthin produced, suggesting that this linker is not compatible with crtZ enzymatic activity. This result is unlikely to be due to a full cleavage of the crtZ-crtY protein since the electrophoresis analysis by SDS-PAGE (Fig. 5C) showed an accumulation of signal migrating at the protein fusion full-length. However, this result needs to be taken with caution. Indeed, the proteins were detectable on SDS-PAGE in the BL21 strain only expressing the plasmid with the protein fusion and not in the strain expressing the four plasmids, probably due to a lower expression level of the enzymes, all under the control of the T7 promoter. Secondly, the strain with SNI01 linker produced a total of 56 mg/L of carotenoids which represents a 40% increase compared to the production in the control strain with independent

enzymes. Finally, the strain with the SHS01 linker displayed a two-fold improvement in the xanthophylls over carotenes ratio compared to the control strain with independent enzymes. This result demonstrated a better conversion of precursors toward the final products, despite a lower amount in total carotenoids. To refine which properties of the linker could explain the different productions observed, the sub criteria of the linker library, i.e., the supposed structure (helical/non-helical) and C-alpha extent were analysed (Fig. 5B). On average, the strains with fused enzymes presented a higher ratio of xanthophylls than the strain with independent enzymes. The strain displaying a linker annotated as helical had a significantly higher xanthophylls ratio than the one having a non-helical (flexible) linker. However, variability in the C-alpha extent of the linker did not yield any significant differences in the ratio of carotenoids produced in the strains. So far, we have demonstrated that both the size and the flexibility of the linker impact the behaviour of the fused enzymes.

3.5. Time-course profile of carotenoids accumulations in strains of interest

To decipher if the improvement of xanthophylls ratio was due to a better enzymatic rate from the crtZ-crtY fusion or to a slower pathway flux, a time-course profile of the accumulation of carotenoid was performed over 24 h. The experiment was carried out for the control strain with independent enzymes, EAB09, the strain with the highest xanthophylls ratio, SHS01, and the strain with the highest amount of total carotenoid, SNI01 (Fig. 6A). In these conditions, the EAB09 strain with independent enzymes accumulated 55% and 12% of lycopene and β-carotene precursors for a final amount of zeaxanthin of 32%. On the contrary, the strain with crtZ-SHS01-crtY enzyme fusion produced up 81% of zeaxanthin with only 7% and 11% of lycopene and β-carotene remaining at the end of reaction. This corresponds to a 9-fold increase in the xanthophylls to carotene ratio. The strain with crtZ-SNI01-crtY fusion had an intermediary profile. Zeaxanthin represented up to 57% of the carotenoids produced, a 1.35-fold improvement compared to the control strain with independent enzymes. The quantity of 70 mg/L obtained here is similar or higher to previous studies in *E. coli* where zeaxanthin was produced up to 51.8 mg/L, 60 mg/L, or 6.33 mg/L (Chen et al., 2021; Li et al., 2015; Wu et al., 2019). However, it could be improved by fermentation processes as fermentation has allowed the production of zeaxanthin to reach 722 mg/L (Shen et al., 2016). The total amount of carotenoids reached 121.7 mg/L, a 1.46-fold increase compare to the strain with independent enzymes. The metabolites fluxes were then calculated for each step of the pathway with $Fl = \frac{\sum A_{m,h} - \sum A_{m,h-1}}{OD_{600,h}}$, where Fl is the flux for a metabolite m, $\sum A_{m,h}$, the sum of the amounts of metabolite m and metabolites derived from m at hour h, $\sum A_{m,h-1}$, the sum of the amounts of metabolite m and metabolites derived from m at hour h-1 and $OD_{600,h}$, the $OD_{600\ nm}$ at hour h (Fig. 6B). All three strains displayed an overall pathway flux increasing overtime (lycopene reaction rate for the strain EAB09 went from 0.315 mg/L/hour/OD at hour 2 post-induction to 1.81 mg/L/hour/OD at hour 16 post-induction), probably due to a progressive accumulation of the crtI in the cell. The SHS01 strain lycopene flux was twice slower than the control strain with independent enzymes at the tenth hour post induction and after 10 h, β-carotene was produced faster than in the control strain. This fluxes pointed out to an acceleration of the step involving crtY, which could be due to its location near the membrane when fused to crtZ, a location known to be favourable to its activity (Yu et al., 2010). We hypothesize that the increase in crtY activity is due to a better location near the membrane. The decrease in the upper pathway flux and increase in the reaction rate of crtY explain the better zeaxanthin selectivity in SHS01 strain. Zeaxanthin production rate was 2.5-fold higher in the SHS01 strain than in the control strain. This could be explained by the increase in the pool of β-carotene, indicating that crtZ enzyme is not limiting. On the contrary, SNI01 strain showed a lycopene flux increased by a 1.4-fold compared to the control strain with independent enzymes. Even with a higher flux, lycopene was not accumulated (Fig. 6A). Indeed, in the SNI01 strain, lycopene was converted to β-carotene more than 3 times faster than in the control strain and zeaxanthin was converted almost 9 times faster in SNI01 than in the control strain (Fig. 6B). The crtZ-crtY fusion with SNI01 linker helps to increase the overall flux in the zeaxanthin pathway, and thus increase the total amount of zeaxanthin.

3.6. Alanine is mainly found at the 1st position of the linker

While the enzyme orientation and the size of the linker were shown to have a crucial effect on the pathway efficiency, no other criteria among the small linkers were shown to impact the performance of the tested fusions. This raised the question of how a variation of such a small peptide (3–5 amino acids), far from the catalytic pockets of the 564 amino acid structure can cause different profile in carotenoids accumulation. The role of the amino acid sequences in small linkers was analysed. Thus, an alignment of the linkers sequences was performed using clustalW. The strains with all the small linkers were then ranged by ascending orders of the xanthophylls to carotenes ratio. Among the crtZ-crtY enzyme fusion strains, the strains with the higher ratio of xanthophylls to carotenes were the ones displaying an alanine or a

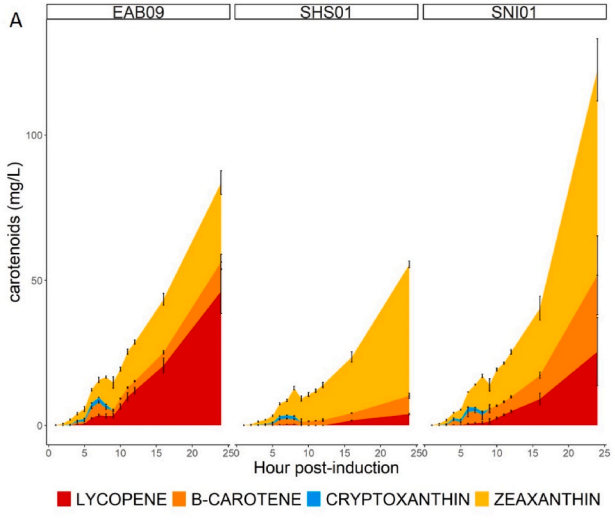

B

HOUR 2

	EAB09	SHS01	SNI01
LYCOPENE	0.315	0.170	0.306
B-CAROTENE	0.315	0.170	0.306
ZEAXANTHIN	0.290	0.170	0.270

HOUR 10

	EAB09	SHS01	SNI01
LYCOPENE	0.543	0.212	0.745
B-CAROTENE	0.178	0.212	0.575
ZEAXANTHIN	0.0689	0.177	0.612

HOUR 16

	EAB09	SHS01	SNI01
LYCOPENE	1.83	1.46	2.49
B-CAROTENE	0.757	1.20	1.80
ZEAXANTHIN	0.599	1.09	1.26

Fig. 6. A: Carotenoid accumulation profile in mg/L of the strains EAB09, SHS01 and SNI01 over time. Errors bars represent the standard deviation of three independent experiments. **B:** Flux of carotenoids at selected time expressed in mg/L/hour/OD_{600nm}. Numbers in green are higher than their control equivalent (EAB09). Numbers in red are lower than their control equivalent (EAB09). (For interpretation of the references to colour in this figure legend, the reader is referred to the Web version of this article.)

glycine at their first position (Fig. 7A). This result was also compared to the set of 1280 linkers found in natural multidomain proteins from the online IBIVU database. Linkers were aligned either by their C-terminal or N-terminal end and the propensity of each amino acid was determined for different positions in the linker. The propensity determined as $Pa = \frac{Nr_{i,p}/\ Nl_p}{\Sigma_i Nr_{i,s}}$, where Pa is the propensity of the amino acid i, $Nr_{i,p}$, the occurrence of the amino acid i at position p, Nl_p, the number of linker and $\sum_i Nr_{i,s}$ the occurrence of the amino acid i in the whole linker set. The results are shown in Fig. 7B. Firstly, it is interesting to note that the first position of the linker, whether at the N-terminal or the C-terminal side, has the most polarized use of amino acid. Indeed, amino acid such as cysteine, tryptophan, phenylalanine, leucine, alanine and valine are overrepresented at the first position whereas amino acid such as the glutamic acid, lysine and arginine are underrepresented. This polarization does not exist at other positions where a more balanced propensity of the amino acids is observed. This result is predictable, as the amino acid in direct contact with the enzyme is expected to bear the highest constraint. On the contrary of the bulky and charged glutamic acid, lysine and arginine, the residues leucine, alanine and valine are rather small hydrophobic and neutral amino acids, which could be more generic as a first residue out of the globular shape of the first enzyme in the natural fusions. Based on the results obtained from the entire database, we could expect that alanine would be more represented than other amino acids in the best linkers from the small linker set, although not more than leucine, phenylalanine or cysteine (see Fig. 8).

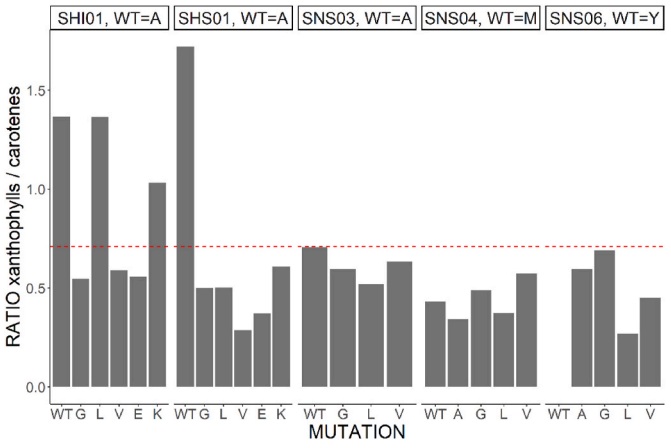

Fig. 8. Ratio of xanthophylls to carotenes produced by crtZ-linker-crtY protein fusion with the five linkers SHI01, SHS01, SNS03, SNS04 and SNS06. The original first amino acid of the linker is indicated at the top of each panel as the Wild-Type (WT) and the ratio of carotenoids in the corresponding strain is represented by the left bar of each panel. Ratio of mutation with amino acids alanine (A), glycine (G), leucine (L), valine (V), glutamic acid (E) and lysine (K) are displayed after the WT left to right. The dashed red line represents the ratio of xanthophylls to carotenes in the strain with independent enzymes. (For interpretation of the references to colour in this figure legend, the reader is referred to the Web version of this article.)

3.7. Alanine is a better amino acid at first position of most linkers

Since the first amino acid of the linker seemed to have an important impact in both the crtZ-crtY fusion construct and natural enzyme fusions, the hypothesis was verified by performing single point mutation of this position. Strains displaying the lowest and highest ratio of xanthophylls over carotenes were selected and the first amino acid of the linker was mutated (Fig. 8). The mutations were made to alanine or glycine, which were shown to be the best in the crtZ-crtY enzyme fusion. Alanine with leucine or valine were also part of the most represented amino acids at the first position of linkers in the database, whereas acid glutamic and lysine were the least represented. Acid glutamic and lysine mutations were only performed on strains SHS01 and SHI01, having a good ratio of xanthophylls in the wild-type (WT) linker.

Mutants to SHS01 and SHI01 strains, which have an alanine as WT amino acid, lose their advantage and revert to a ratio similar to the control strain. SNS03 and SNS04 strains had a similar ratio independently of the nature of their first amino acid, indicating that amino acids in other positions also impact the protein fusion. Surprisingly, the profile of the SNS06 strain was completely reverted with the single mutation. The strain which was not producing xanthophylls with the tyrosine at its first position had a ratio close to the control strain with independent enzymes with an alanine or glycine. The reversion also happened with

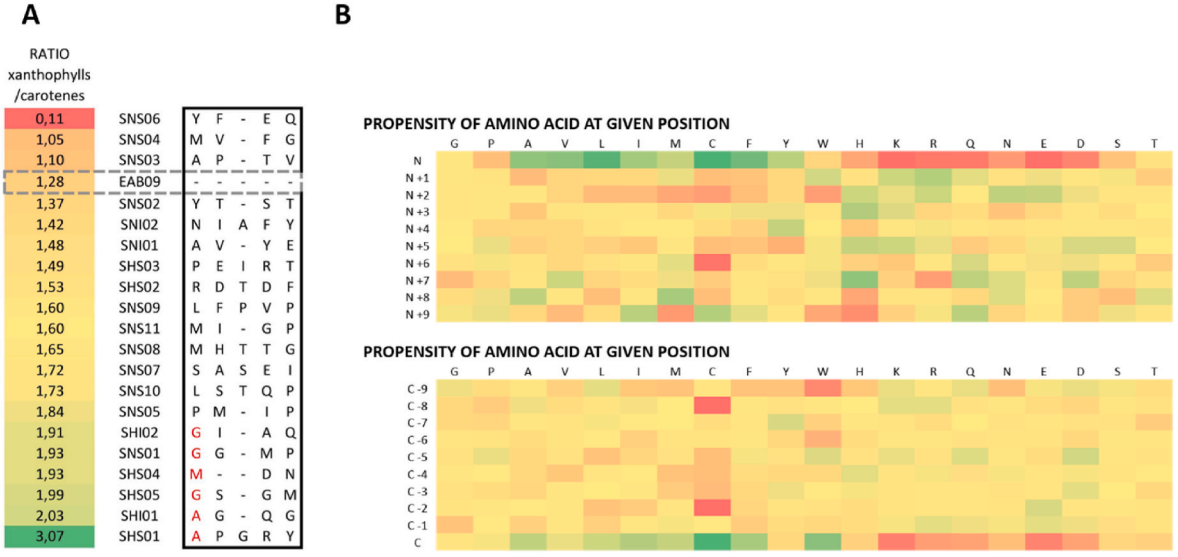

Fig. 7. A: Sequence alignment of small linkers depicted in Fig. 5. The dashed frame surrounds the independent enzymes. The linker sequences are framed by a plain line box. Constructions are ranged based on the ratio of xanthophylls to carotenes accumulated in the strains. Alignment performed with clustalW. **B:** Amino acid propensity by position in the linker based on the 1280 linkers from the online database. Propensity values are represented as a red to green colour gradient, from smaller to higher values, respectively. Top panel represents position 1 to 10 of linkers from the N-terminal. Bottom panel represents last ten residues of linkers. First raw of table is the one letter code for amino acid. (For interpretation of the references to colour in this figure legend, the reader is referred to the Web version of this article.)

leucine and valine mutants, although to a lower extent. The tyrosine at the first position of SNS06 linker cannot be entirely responsible of the lack of xanthophylls in the strain. Indeed, the enzyme fusion in the SNS02 strain also has a tyrosine at the first position of the linker, and this strain does produce xanthophylls. Overall, looking at the carotenoid ratio in the crtZ-crtY enzyme fusion, in certain cases, alanine seems to be the best amino acid for the first position of the linker, and in other cases, glycine or valine are equally good or even better. However, adjustment to the first amino acid of the linker is not enough to change the crtZ-crtY fusion into one accumulating xanthophylls.

4. Discussion

Expressing the zeaxanthin pathway in *E. coli* leads to a partial conversion of β-carotene into zeaxanthin. To improve the overall bioprocess, the two enzymes crtY and crtZ catalysing the bottleneck metabolic steps were fused using a linker library. By successively adjusting different linker criteria between crtZ and crtY enzymes, the impact of the enzyme orientation and linker size were shown to be crucial for the performance of the crtZ-crtY enzyme. CrtY was only efficient when placed at the C-terminal of the enzyme fusion and crtZ at the N-terminal of the enzyme fusion as it was demonstrated in previous studies (Ding et al., 2022; Wu et al., 2019). We speculated that it could be explain by the orientation of both enzyme around the membrane. CrtZ is predicted to be membrane bound and crtY membrane-associated and this could require more or less flexibility to achieve an optimal configuration allowing the enzyme to reach the hydrophobic substrate embedded in the cell membrane. By testing a library of linkers with a large diversity, small linkers of three to four amino acids were found to give strains more efficient than those with larger linkers, and than the independent enzymes in 85% of the cases. Among the linkers tested, some linker sequences led to specific phenotypes. In particular, the crtZ-crtY enzyme fusion with SHS01 linker gave a strain with a 9-fold improvement of the xanthophylls over carotene ratio when compared to the strain with independent enzymes. The enzyme fusion with SNI01 linker allowed a 1.46-fold increase of the pathway flux. Some improvements of the enzyme fusion might be due to a higher expression of crtZ when fused to crtY. Unfortunately, efforts to quantify the crtY, crtZ or crtZ-crtY protein using western-blot remained unsuccessful, probably due to the membrane bound/associated behaviour of the enzyme complexes. Gathering enzyme domains using a linker enforces a 1:1 ratio of the enzymes that might not be the same when the enzymes are independent from each other and which affects the overall metabolites distribution, as seen in the strains SHS01, SNS06 and SNI01. On top of the physical parameters of the linker involved in the efficiency of the fusion, the sequence of the linker was also a determinant criterion, with the first amino acid of the sequence being crucial, both in natural enzymes and crtZ-crtY fusions. Exploring the idiosyncrasy of linkers can allow to fine-tune an enzyme fusion and this approach can be used on any model due to the versatility of the method.

While the fusion strategy is simple to implement, the linker sequences to explore leads to a time-consuming process. To narrow the sequences to explore, our study and others (Guo et al., 2017; Li et al., 2016) suggest that a good approach to fuse enzymes is to assay the two enzyme orientations using the flexible motif GGGGS or the rigid spacer EAAAK and tune the first amino acid of the most efficient assembly.

However, the improvement obtained by enzyme fusion is often limited, with an improvement range often between 1 and 5-fold (Bakkes et al., 2015; Baklouti et al., 2020; Wang et al., 2021). In the recent years, several studies (Kuzmak et al., 2019; Poshyvailo et al., 2017; Rabe et al., 2017; Wheeldon et al., 2016) showed that enzyme proximity could only enhanced cascade reaction temporarily (order of millisecond before steady state) as diffusion is fast compared with usual catalytic reaction rates and benefits can only be seen in presence of a competing reaction. Moreover, the imposed stoichiometry of active sites in enzymes fusion implies that the slowest reaction will limit the overall activity. To overcome this limitation, enzyme clusters using post-translational assembly or scaffold assembly can remove this constraint by compensating the different reaction rate and adjusting enzyme stoichiometry. Overall, enzymatic assembly is just one of the tools of metabolic engineering and should be combined with others, such as enzymatic engineering. Obtaining more efficient individual enzymes could then present a synergic efficiency when embedded into enzymatic complexes.

In this study, the β-carotene cyclase crtY and the β-carotene hydroxylase crtZ were fused. A collection of linkers was used to fine-tune the enzyme fusion and the role of linker size and structure was demonstrated in this specific set of proteins. Moreover, we showed for the first time that the amino acids at the extremities of the linker in contact with the enzymes have a higher selection constraint than amino acid in other position. In the end, we obtained the SNI01 strain with a 1.46-fold increase of the pathway flux and the SHS01 strain with a 9-fold increase in the ratio of xanthophylls produced. Our linker library approach can be implemented for any protein fusion.

Author contributions

Aurélie Bouin: Conceptualization, Investigation, Writing - Original Draft; **Congqiang Zhang**: Conceptualization, Writing (review and editing), Funding acquisition: **Nic D Lindley**: Conceptualization, Writing (review and editing), Funding acquisition; **Gilles Truan**: Conceptualization, Writing (review and editing), Funding acquisition; **Thomas Lautier**: Conceptualization, Writing (review and editing), supervision, Funding acquisition.

Funding

In the frame of the France-Singapore International Research Program in Synthetic Biology for a Bio-inspired Economy, this research was funded by the National Research Foundation, Prime Minister's Office, Singapore under its Campus for Research Excellence and Technological Enterprise (CREATE) EcoCTs project and by the Biotrans IAF-PP (HBMS Domain): H17/01/a0/006. The 2019 AME Young Investigator Research Grant (YIRG) A2084c0064 awarded to CZ supported the laboratory enzymes and carotenoid standards for this project. AB PhD grant was cofounded by the MICA division of the French National Research Institute for Agriculture, Food and the Environment and by the Singaporean A*STAR research attachment programme.

Declaration of competing interest

The authors declare that they have no known competing financial interests or personal relationships that could have appeared to influence the work reported in this paper.

Data availability

Data will be made available on request.

Appendix A. Supplementary data

Supplementary data to this article can be found online at https://doi.org/10.1016/j.mec.2023.e00222.

References

Argos, P., 1990. An investigation of oligopeptides linking domains in protein tertiary structures and possible candidates for general gene fusion. J. Mol. Biol. 211, 943–958. https://doi.org/10.1016/0022-2836(90)90085-Z.

Arunkumar, R., Gorusupudi, A., Bernstein, P.S., 2020. The macular carotenoids: a biochemical overview. Biochim. Biophys. Acta BBA - Mol. Cell Biol. Lipids 1865, 158617. https://doi.org/10.1016/j.bbalip.2020.158617.

Bakkes, P.J., Biemann, S., Bokel, A., Eickholt, M., Girhard, M., Urlacher, V.B., 2015. Design and improvement of artificial redox modules by molecular fusion of

flavodoxin and flavodoxin reductase from Escherichia coli. Sci. Rep. 5, 12158 https://doi.org/10.1038/srep12158.
Baklouti, Z., Delattre, C., Pierre, G., Gardarin, C., Abdelkafi, S., Michaud, P., Dubessay, P., 2020. Biochemical characterization of a bifunctional enzyme constructed by the fusion of a glucuronan lyase and a chitinase from trichoderma sp. Life 10, 234. https://doi.org/10.3390/life10100234.
Barreiro, C., Barredo, J.-L., 2018. Carotenoids production: a healthy and profitable industry. In: Barreiro, C., Barredo, J.-L. (Eds.), Microbial Carotenoids, Methods in Molecular Biology. Springer New York, New York, NY, pp. 45–55. https://doi.org/10.1007/978-1-4939-8742-9_2.
Bouvier, F., Keller, Y., 1998. Xanthophyll Biosynthesis: Molecular and Functional Characterization of Carotenoid Hydroxylases from Pepper Fruits žCapsicum Annuum L./9.
Breitenbach, J., Pollmann, H., Sandmann, G., 2019. Genetic modification of the carotenoid pathway in the red yeast Xanthophyllomyces dendrorhous: engineering of a high-yield zeaxanthin strain. J. Biotechnol. 289, 112–117. https://doi.org/10.1016/j.jbiotec.2018.11.019.
Carquet, M., Pompon, D., Truan, G., 2015. Transcription interference and ORF nature strongly affect promoter strength in a reconstituted metabolic pathway. Front. Bioeng. Biotechnol. 3.
Chen, X., Lim, X., Bouin, A., Lautier, T., Zhang, C., 2021. High-level de novo biosynthesis of glycosylated zeaxanthin and astaxanthin in Escherichia coli. Bioresour. Bioprocess. 8, 67. https://doi.org/10.1186/s40643-021-00415-0.
Ding, Y.-W., Lu, C.-Z., Zheng, Y., Ma, H.-Z., Jin, J., Jia, B., Yuan, Y.-J., 2022. Directed evolution of the fusion enzyme for improving astaxanthin biosynthesis in Saccharomyces cerevisiae. Synth. Syst. Biotechnol. 8, 46–53. https://doi.org/10.1016/j.synbio.2022.10.005.
Elleuche, S., 2015. Bringing functions together with fusion enzymes—from nature's inventions to biotechnological applications. Appl. Microbiol. Biotechnol. 99, 1545–1556. https://doi.org/10.1007/s00253-014-6315-1.
George, R.A., Heringa, J., 2002. An analysis of protein domain linkers: their classification and role in protein folding. Protein Eng. 15, 871–879. https://doi.org/10.1093/protein/15.11.871.
Geraldi, A., Khairunnisa, F., Farah, N., Bui, L.M., Rahman, Z., 2021. Synthetic scaffold systems for increasing the efficiency of metabolic pathways in microorganisms. Biology 10, 216. https://doi.org/10.3390/biology10030216.
Gräwe, A., Ranglack, J., Weyrich, A., Stein, V., 2020. iFLinkC: an iterative functional linker cloning strategy for the combinatorial assembly and recombination of linker peptides with functional domains. Nucleic Acids Res. 48, e24. https://doi.org/10.1093/nar/gkz1210 e24.
Guo, H., Yang, Y., Xue, F., Zhang, H., Huang, T., Liu, W., Liu, H., Zhang, F., Yang, M., Liu, C., Lu, H., Zhang, Y., Ma, L., 2017. Effect of flexible linker length on the activity of fusion protein 4-coumaroyl-CoA ligase::stilbene synthase. Mol. Biosyst. 13, 598–606. https://doi.org/10.1039/c6mb00563b.
Henke, N.A., Wendisch, V.F., 2019. Improved astaxanthin production with corynebacterium glutamicum by application of a membrane fusion protein. Mar. Drugs 17. https://doi.org/10.3390/md17110621.
Krubasik, P., Sandmann, G., 2000. Molecular evolution of lycopene cyclases involved in the formation of carotenoids with ionone end groups. Biochem. Soc. Trans. 28.
Kuzmak, A., Carmali, S., Lieres, E. von, Russell, A.J., Kondrat, S., 2019. Can enzyme proximity accelerate cascade reactions? Sci. Rep. 9 https://doi.org/10.1038/s41598-018-37034-3.
Li, G., Huang, Z., Zhang, C., Dong, B.J., Guo, R.H., Yue, H.W., Yan, L.T., Xing, X.H., 2016. Construction of a linker library with widely controllable flexibility for fusion protein design. Appl. Microbiol. Biotechnol. 100, 215–225. https://doi.org/10.1007/s00253-015-6985-3.
Li, M., Hou, F., Wu, T., Jiang, X., Li, F., Liu, H., Xian, M., Zhang, H., 2020. Recent advances of metabolic engineering strategies in natural isoprenoid production using cell factories. Nat. Prod. Rep. 37, 80–99. https://doi.org/10.1039/c9np00016j.
Li, X.R., Tian, G.Q., Shen, H.J., Liu, J.Z., 2015. Metabolic engineering of Escherichia coli to produce zeaxanthin. J. Ind. Microbiol. Biotechnol. 42, 627–636. https://doi.org/10.1007/s10295-014-1565-6.
Mackenzie, J.S., Jeggo, M., 2019. The one health approach—why is it so important? Trav. Med. Infect. Dis. 4, 88. https://doi.org/10.3390/tropicalmed4020088.
Madeira, F., Park, Y. mi, Lee, J., Buso, N., Gur, T., Madhusoodanan, N., Basutkar, P., Tivey, A.R.N., Potter, S.C., Finn, R.D., Lopez, R., 2019. The EMBL-EBI search and sequence analysis tools APIs in 2019. Nucleic Acids Res. 47, W636–W641. https://doi.org/10.1093/nar/gkz268.
Mares, J., 2016. Lutein and zeaxanthin isomers in eye health and disease. Annu. Rev. Nutr. 36, 571–602. https://doi.org/10.1146/annurev-nutr-071715-051110.
Nishizaki, T., Tsuge, K., Itaya, M., Doi, N., Yanagawa, H., 2007. Metabolic engineering of carotenoid biosynthesis in Escherichia coli by ordered gene assembly in Bacillus subtilis. Appl. Environ. Microbiol. 73, 1355–1361. https://doi.org/10.1128/AEM.02268-06.
Nogueira, M., Enfissi, E.M.A., Welsch, R., Beyer, P., Zurbriggen, M.D., Fraser, P.D., 2019. Construction of a fusion enzyme for astaxanthin formation and its characterisation in microbial and plant hosts: a new tool for engineering ketocarotenoids. Metab. Eng. 52, 243–252. https://doi.org/10.1016/j.ymben.2018.12.006.
Norris, J.L., Hughes, R.M., 2018. protaTETHER – a method for the incorporation of variable linkers in protein fusions reveals impacts of linker flexibility in a PKAc-GFP fusion protein. FEBS Open Bio 8, 1029–1042. https://doi.org/10.1002/2211-5463.12414.
Oliveira, S., Malinowsky, C., M.Tomazzoli, M., Uarrota, V., Yunes, R., Maraschin, M., 2013. Development of extraction process of the xanthophylls lutein and zeaxanthin from brazillian maize (zea mays L.) landraces. p.610. https://doi.org/10.5301/EJO.2013.11169.
Park, S.Y., Eun, H., Lee, M.H., Lee, S.Y., 2022. Metabolic engineering of Escherichia coli with electron channelling for the production of natural products. Nat. Catal. 5, 726–737. https://doi.org/10.1038/s41929-022-00820-4.
Pollmann, H., Breitenbach, J., Sandmann, G., 2017. Engineering of the carotenoid pathway in Xanthophyllomyces dendrorhous leading to the synthesis of zeaxanthin. Appl. Microbiol. Biotechnol. 101, 103–111. https://doi.org/10.1007/s00253-016-7769-0.
Poshyvailo, L., Lieres, E. von, Kondrat, S., 2017. Does metabolite channeling accelerate enzyme-catalyzed cascade reactions? PLoS One 12, e0172673. https://doi.org/10.1371/journal.pone.0172673.
Qiu, X., Xie, S.-S., Min, L., Wu, X.-M., Zhu, L.-Y., Zhu, L., 2018. Spatial organization of enzymes to enhance synthetic pathways in microbial chassis: a systematic review. Microb. Cell Factories 17, 120. https://doi.org/10.1186/s12934-018-0965-0.
Rabe, K.S., Müller, J., Skoupi, M., Niemeyer, C.M., 2017. Cascades in compartments: en route to machine-assisted biotechnology. Angew. Chem. Int. Ed. 56, 13574–13589. https://doi.org/10.1002/anie.201703806.
Rabeharindranto, H., Castaño-Cerezo, S., Lautier, T., Garcia-Alles, L.F., Treitz, C., Tholey, A., Truan, G., 2019. Enzyme-fusion strategies for redirecting and improving carotenoid synthesis in S. cerevisiae. Metab. Eng. Commun. 8, 1–11. https://doi.org/10.1016/j.mec.2019.e00086.
Rinaldi, M.A., Ferraz, C.A., Scrutton, N.S., 2022. Alternative metabolic pathways and strategies to high-titre terpenoid production in *Escherichia coli*. Nat. Prod. Rep. 39, 90–118. https://doi.org/10.1039/D1NP00025J.
Sadaf, A., Mortensen, J.S., Capaldi, S., Tikhonova, E., Hariharan, P., Ribeiro, O., Loland, C.J., Guan, L., Byrne, B., Chae, P.S., 2016. A class of rigid linker-bearing glucosides for membrane protein structural study. Chem. Sci. 7, 1933–1939. https://doi.org/10.1039/c5sc02900g.
Sajilata, M.G., Singhal, R.S., Kamat, M.Y., 2008. The carotenoid pigment zeaxanthin—a review. Compr. Rev. Food Sci. Food Saf. 7, 29–49. https://doi.org/10.1111/j.1541-4337.2007.00028.x.
Shen, H.J., Cheng, B.Y., Zhang, Y.M., Tang, L., Li, Z., Bu, Y.F., Li, X.R., Tian, G.Q., Liu, J. Z., 2016. Dynamic control of the mevalonate pathway expression for improved zeaxanthin production in Escherichia coli and comparative proteome analysis. Metab. Eng. 38, 180–190. https://doi.org/10.1016/j.ymben.2016.07.012.
Van Rosmalen, M., Krom, M., Merkx, M., 2017. Tuning the flexibility of glycine-serine linkers to allow rational design of multidomain proteins. Biochemistry 56, 6565–6574. https://doi.org/10.1021/acs.biochem.7b00902.
Wang, X., Pereira, J.H., Tsutakawa, S., Fang, X., Adams, P.D., Mukhopadhyay, A., Lee, T. S., 2021. Efficient production of oxidized terpenoids via engineering fusion proteins of terpene synthase and cytochrome P450. Metab. Eng. 64, 41–51. https://doi.org/10.1016/j.ymben.2021.01.004.
Wheeldon, I., Minteer, S.D., Banta, S., Barton, S.C., Atanassov, P., Sigman, M., 2016. Substrate channelling as an approach to cascade reactions. Nat. Chem. 8, 299–309. https://doi.org/10.1038/nchem.2459.
Wriggers, W., Chakravarty, S., Jennings, P.A., 2005. Control of protein functional dynamics by peptide linkers. Biopolym. - Pept. Sci. Sect. 80, 736–746. https://doi.org/10.1002/bip.20291.
Wu, Z., Zhao, D., Li, S., Wang, J., Bi, C., Zhang, X., 2019. Combinatorial modulation of initial codons for improved zeaxanthin synthetic pathway efficiency in Escherichia coli. Microbiol. 1–22 https://doi.org/10.1002/mbo3.930.
Xie, Y., Chen, S., Xiong, X., 2021. Metabolic engineering of non-carotenoid-producing yeast Yarrowia lipolytica for the biosynthesis of zeaxanthin. Front. Microbiol. 12, 699235 https://doi.org/10.3389/fmicb.2021.699235.
Yu, Q., Schaub, P., Ghisla, S., Al-Babili, S., Krieger-Liszkay, A., Beyer, P., 2010. The lycopene cyclase CrtY from Pantoea ananatis (formerly erwinia uredovora) catalyzes an FADred-dependent non-redox reaction. J. Biol. Chem. 285, 12109–12120. https://doi.org/10.1074/jbc.M109.091843.
Zafar, J., Aqeel, A., Shah, F.I., Ehsan, N., Gohar, U.F., Moga, M.A., Festila, D., Ciurea, C., Irimie, M., Chicea, R., 2021. Biochemical and immunological implications of lutein and zeaxanthin. Int. J. Mol. Sci. 22, 10910 https://doi.org/10.3390/ijms222010910.
Zakynthinos, G., Varzakas, T., 2016. Carotenoids: from plants to food industry. Curr. Res. Nutr. Food Sci. J. 4, 38–51. https://doi.org/10.12944/CRNFSJ.4.Special-Issue1.04.
Zhang, C., Chen, X., Lindley, N.D., Too, H.P., 2018a. A "plug-n-play" modular metabolic system for the production of apocarotenoids. Biotechnol. Bioeng. 115, 174–183. https://doi.org/10.1002/bit.26462.
Zhang, C., Seow, V.Y., Chen, X., Too, H.P., 2018b. Multidimensional heuristic process for high-yield production of astaxanthin and fragrance molecules in Escherichia coli. Nat. Commun. 9, 1–12. https://doi.org/10.1038/s41467-018-04211-x.
Zhang, Y., Liu, Z., Sun, J., Xue, C., Mao, X., 2018. Biotechnological production of zeaxanthin by microorganisms. Trends Food Sci. Technol. 71, 225–234. https://doi.org/10.1016/j.tifs.2017.11.006.